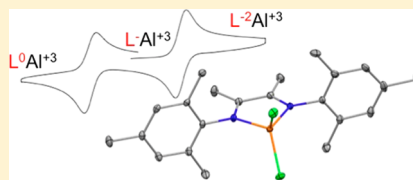


Synthesis and Characterization of Aluminum- α -diimine Complexes over Multiple Redox StatesBren E. Cole,[†] Jeffrey P. Wolbach,[†] William G. Dougherty, Jr.,[‡] Nicholas A. Piro,[‡] W. Scott Kassel,[‡] and Christopher R. Graves^{*†}[†]Department of Chemistry & Biochemistry, Albright College, 13th & Bern Street, Reading, Pennsylvania 19612, United States[‡]Department of Chemistry, Villanova University, 800 Lancaster Avenue, Villanova, Pennsylvania 19085, United States

Supporting Information

ABSTRACT: The aluminum complexes (L_{Mes}^{2-})AlCl(THF) (**3**) and (L_{Dipp}^-)AlCl₂ (**4**) ($L_{Mes} = N,N'$ -bis[2,4,6-trimethylphenyl]-2,3-dimethyl-1,4-diazabutadiene, $L_{Dipp} = N,N'$ -bis[2,6-diisopropylphenyl]-2,3-dimethyl-1,4-diazabutadiene) were prepared by direct reduction of the ligands with sodium metal followed by salt metathesis with AlCl₃. The (L_{Mes}^-)AlCl₂ (**5**) complex was prepared through one-electron oxidative functionalization of **3** with either AgCl or CuCl. Complex **3** was characterized using ¹H and ¹³C NMR spectroscopies. Single-crystal X-ray diffraction analysis of the complexes revealed that **3–5** are all four-coordinate, with **3** exhibiting a trigonal pyramidal geometry, while **4** and **5** exist between trigonal pyramidal and tetrahedral. Notable in the L_{Mes} complexes **3** and **5** is a systematic lengthening of the C–N_{imido} bonds and shortening of the C–C bond in the N–C–C–N backbone with increased electron density on the ligand. The geometries of the complexes **3** and **5** were optimized using DFT, which showed primarily ligand-based frontier orbitals, supporting the analysis of the solid-state structural data. The complexes **3–5** were also characterized by electrochemistry. The cyclic voltammogram of complex **3** showed an oxidation processes at –0.94 and –0.03 V versus ferrocene, while complexes **4** and **5** exhibit both reduction (–1.37 and –1.34 V, respectively) and oxidation (–0.62 and –0.73 V, respectively) features.



INTRODUCTION

A central challenge in chemistry is the need to develop catalytic systems for small-molecule transformations that employ nonprecious metal complexes.¹ Aluminum is an attractive choice for such catalyst development because it is readily available, inexpensive, and nontoxic.² Aluminum constitutes ~8% of the mass of the earth's crust,³ and at ~\$2.00/kg,⁴ aluminum is ~10⁴–10⁵ times less expensive than precious metals such as Pd, Pt, Rh, and Ir.⁵ Although aluminum complexes have a rich history in Lewis-acid catalysis,⁶ application of aluminum complexes as reagents for the electrophilic activation and redox transformation of small molecules is in its infancy.

Aluminum chemistry has historically been defined by the stability of the tripositive configuration.³ The lack of readily accessible multielectron redox states has limited the applicability of Al complexes as catalytic species for processes dependent on oxidative and reductive transformations. Roesky and co-workers have prepared low-valent Al(I)-carbene analogues and reported the two-electron redox chemistry of the complexes.^{7–9} This work clearly demonstrates that when a redox process is available, the aluminum center is capable of facilitating small-molecule activation coupled with redox transformations. However, molecular complexes supporting low-valent Al(I) are not common, with only a handful of known examples.^{10–15} Additionally, although the Al(I) → Al(III) oxidation reaction is facile, the corresponding Al(III) → Al(I) reduction occurs only under highly reducing conditions. This presents difficulties in the regeneration of Al(I) after

reaction to Al(III), inhibiting the application of the Al(I)/Al(III) couple in practical catalysis. In order for aluminum complexes to be applicable for redox transformations, complexes able to readily undergo reversible oxidation and reduction chemistries are required.

Metal complexes of redox-active ligands are a burgeoning class of compounds that have been used to great success for multielectron transformations in recent years.^{16–18} Recent work by Berben and co-workers has demonstrated that coordination of iminopyridine-based ligands (IP) to an Al(III) ion results in a series of complexes spanning multiple oxidation states. When utilizing iminopyridine ligands with an unsubstituted pyridine ring, complexes of the type (IP)AlX₃, (IP[–])₂AlX, and [M][(IP^{2–})₂Al] (X = monoanionic ligand; M = Na(THF)₆, Na(DME)₃, NBu₄) were prepared.^{19–21} Increasing the steric demand of the IP ligand through substitution of the pyridine ring resulted in a series of complexes with just one IP ligand: (IP[–])AlX₂ and (IP^{2–})AlX(OEt₂) (X = Cl, Me).²² The complexes exhibit multiple redox couples in their cyclic voltammograms, demonstrating that the redox characteristics of the ligand were extended to the complexes. Berben also demonstrated that the redox behavior could be exploited to facilitate reactivity at the Al(III) ion,^{19,20} including reduction of CO₂ into CO₃^{2–}.²³ This work demonstrates that incorporation of ligands that can access several redox states can result in aluminum(III) complexes capable of redox properties and that

Received: February 18, 2014

Published: March 24, 2014

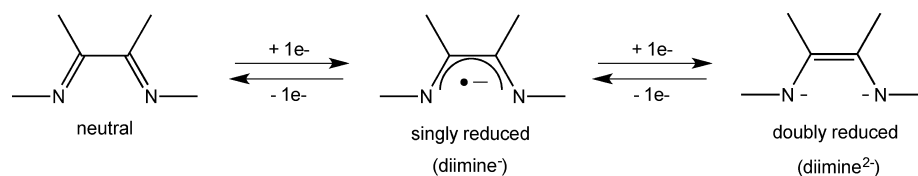


Figure 1. Redox states of the α -diimine ligand.

the redox activity can be harnessed for novel reaction chemistry.

We have been investigating the coordination chemistry of the classical redox-active ligands α -diimines with aluminum(III). α -Diimines are well known to exhibit rich redox behavior²⁴ and can be singly or doubly reduced to form the mono- (diimine⁻) and dianionic (diimine²⁻) species, respectively (Figure 1). Various main group,²⁵ transition,²⁶ and rare earth-metal²⁷ complexes incorporating α -diimines across all three ligand oxidation states have been reported. The α -diimine ligands are attractive, as both the steric and electronic properties of the ligand can be readily modified through variation of the carbon and nitrogen substituents in the N–C–N backbone. Tunability of the ligand through substituent effects provides a large parameter space for optimization of the aluminum complexes.

The coordination chemistry of α -diimine ligands to aluminum(III) has some precedent. Raston and collaborators have reported the oxidation of aluminum metal with the ^tBu–DAB (^tBu–DAB = *N,N'*-di(*tert*-butyl)-1,4-diazabutadiene) ligand to give the complex Al(^tBu–DAB)₂.²⁸ Physical characterization of the complex revealed the electronic structure of the complex to be best described as an aluminum(III) ion coordinated by a doubly reduced ^tBu–DAB²⁻ ligand and another ^tBu–DAB⁻ singly reduced radical anion. The Murphy group has prepared aluminum complexes of the related ligand Dipp–DAB (Dipp–DAB = *N,N'*-bis(2,6-diisopropylphenyl)-1,4-diazabutadiene).²⁹ Reaction of Dipp–DAB with a 1:2 mixture of AlI₃ and Al metal gives (Dipp–DAB⁻)AlI₂, while reaction of the ligand with just AlI₃ gives [(Dipp–DAB)AlI₂][I]. Aluminum complexes with the related Dipp–BIAN ligand (Dipp–BIAN = 1,2-bis(2,6-diisopropylphenylimino)acenaphthylene) have also been prepared for both the mono- and dianionic forms of the ligand. Fedushkin and co-workers synthesized compounds with the singly reduced ligand of the type (Dipp–BIAN⁻)AlX₂, where X = Cl³⁰ or an alkyl group (Me, Et, or ^tBu).³¹ The analogous [Mg₂Cl₃(THF)₆][(Dipp–BIAN²⁻)AlCl₂] compound was also prepared.³⁰ Recently, Cui and co-workers reported the reaction of the protonated ene-diamide Ar–NH–C(CH₃)=C(CH₃)–NH–Ar (Ar = 2,4-*i*Pr₂–C₆H₃, L_{Dipp}H₂) with trialkylaluminum compounds.³² Reaction of L_{Dipp}H₂ with AlMe₃ gave the (L_{Dipp}H)AlMe₂ compound, while the analogous reaction with AlEt₃ gave (L_{Dipp}⁻)AlEt₂.

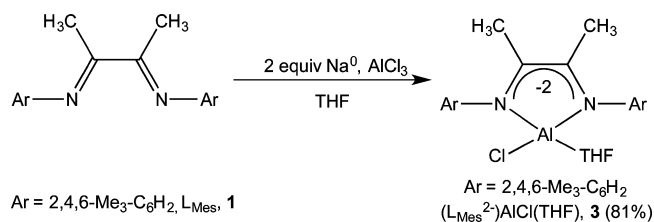
However, a comprehensive structural, electrochemical, and quantum chemistry study of Al- α -diimine complexes has not been demonstrated. Herein we report the synthesis and characterization of aluminum complexes supported by *N*-aryl-substituted α -diimine ligands of the type Ar–N=C(CH₃)–C(CH₃)=N–Ar (Ar = 2,4,6-Me₃-C₆H₂, L_{Mes}, **1**; Ar = 2,6-*i*Pr₂-C₆H₃, L_{Dipp}, **2**). We have prepared and characterized Al- α -diimine complexes with both the singly and doubly reduced form of the ligands and characterized them, including a quantum chemical description of the compounds. Importantly, the cyclic voltammograms of the complexes exhibit reversible

redox properties, indicating that the redox properties of the ligand are also present in the complexes.

RESULTS AND DISCUSSION

Synthesis of Aluminum Complexes 3–5. The aluminum complex incorporating the doubly reduced α -diimine ligand L_{Mes} (**1**) was prepared on a 1 g scale. Reduction of **1** with 2 equiv of alkali metal in THF followed by addition of AlCl₃ and stirring at room temperature for 12 h afforded (L_{Mes}²⁻)AlCl(THF) (**3**) as an off-white solid in 81% isolated yield after

Scheme 1. Synthesis of the Al- α -diimine Doubly Reduced Complex (L_{Mes}²⁻)AlCl(THF) (**3**)

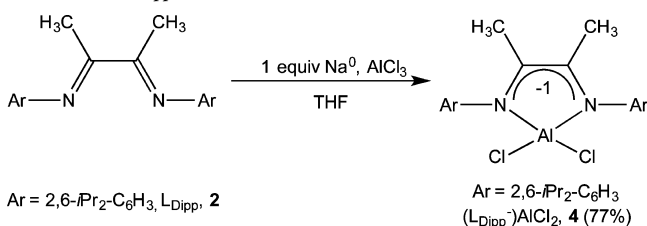


workup (Scheme 1). Complex **3** was readily characterized by ¹H and ¹³C NMR spectroscopies, with the spectra indicating **3** is a diamagnetic complex. The *ortho*-methyl groups of complex **3** are symmetry inequivalent and broadened ($\Delta\nu_{1/2} = 71$ and 86 Hz) at 25 °C in its ¹H NMR spectra, suggesting a hindered rotation about the N–C_{Ar} bond. VT-NMR shows that the two signals coalesce above 60 °C (see Figure S2). Although **3** can be stored under nitrogen at –25 °C for several weeks without noticeable degradation, the compound does slowly decompose and cannot be indefinitely stored.

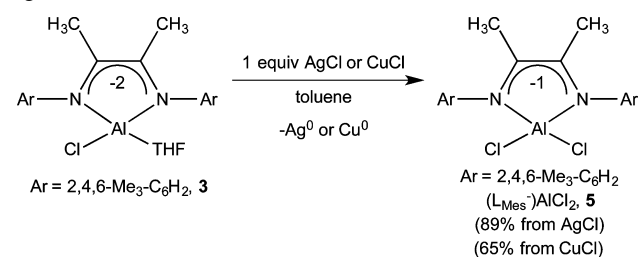
Attempts to prepare the corresponding (L_{Dipp}²⁻)AlCl(THF) complex using a similar pathway to that for **3** implementing the L_{Dipp} (**2**) ligand proved unsuccessful, resulting in intractable mixtures of products. Increasing the amount to 4 equiv or changing the identity (K versus Na) of the alkali-metal reducing agent did not lead to an improved reaction outcome. However, a direct reduction route could be employed successfully for the synthesis of the singly reduced complex: Reduction of **2** with 1 equiv of sodium metal followed by addition of AlCl₃ and stirring at room temperature for 12 h afforded (L_{Dipp}⁻)AlCl₂ (**4**) in 77% yield (Scheme 2).

A similar pathway to directly prepare the singly reduced (L_{Mes}⁻)AlCl₂ complex **5** through limiting the amount of alkali metal employed to 1 equiv yielded multiple products, including both the doubly and singly reduced complexes and free ligand. However, as shown in Scheme 3, reaction of **3** with 1 equiv of AgCl resulted in oxidative functionalization to give (L_{Mes}⁻)AlCl₂ (**5**) as an orange solid in 89% yield. Compound **5** could also be prepared using CuCl as the oxidant; reaction of **3** with 1 equiv of CuCl gave **5** in 65% yield. Although the AgCl reaction was run for 12 h, the CuCl reaction was stopped after 3 h, as

Scheme 2. Synthesis of the Al- α -diimine Singly Reduced Complex (L_{Dipp}^-)AlCl₂ (4)



Scheme 3. Synthesis of Al- α -diimine Singly Reduced Complex (L_{Mes}^-)AlCl₂ (5) through Oxidative Functionalization with M-Cl (M = Ag, Cu) Oxidizing Agents



longer reaction times resulted in decreased yields and impure product. These oxidative functionalization routes demonstrate that the redox properties of the complex can be coupled to reaction chemistry at the aluminum ion. Similar reaction chemistry was observed by the Berben group, who showed that their reduced Al-iminopyridine complex [Na(THF)₆]-[(IP²⁻)₂Al] could be oxidatively functionalized using ZnX₂ compounds to (IP⁻)₂AlX (X = Cl, CPh, N₃, SPh, NPh).²⁰ Both complexes 4 and 5 are paramagnetic with a singly reduced ligand and result in ¹H NMR spectra that display no signals (Figures S4 and S5).

Attempts to prepare aluminum complexes with neutral L_{Mes} and L_{Dipp} ligands were unsuccessful. Reaction between 1 or 2 with AlCl₃ did not yield the LAICl₃ adducts, and reaction of complex 4 or 5 with either AgCl or CuCl resulted in isolation of free neutral diimine ligands. Finally, reaction of 5 with FcBPh₄ in THF produced free L_{Mes} ligand, [trans-(THF)₄AlCl₂][BPh₄]₃ and ferrocene. These results suggest that L_{Mes} and L_{Dipp} do not effectively bind the Al^{III} cation in their neutral forms in the presence of coordinating solvent.³⁴

Solid-State Structures of 3–5. The structures of the complexes 3–5 were corroborated by X-ray crystallography. Single crystals of 3 were grown from a toluene solution at –25 °C, which crystallized with a molecule of interstitial toluene (Figure 2). Single crystals of 4 and 5 were both grown from hexane solutions at –25 °C (Figures 3 and 4). Crystallographic data are provided in Table 1, and selected bonding metrics for the complexes are provided in Table 2.

All three complexes 3–5 are four-coordinate at the aluminum(III) cation, with a bidentate α -diimine ligand and two monodentate ligands (either Cl or THF) constituting the coordination sphere. According to the τ_4 parameter introduced by Houser,³⁵ the geometry of 3 is best described as trigonal pyramidal with $\tau_4 = 0.82$. Conversely, 4 and 5 have τ_4 values of 0.92 and 0.90, respectively, and exist between the trigonal pyramidal and tetrahedral geometries. At 2.1078(6)–2.1278(6) Å, the Al–Cl bond lengths for the complexes are unremarkable and are in the range of other terminal Al–Cl bonds reported

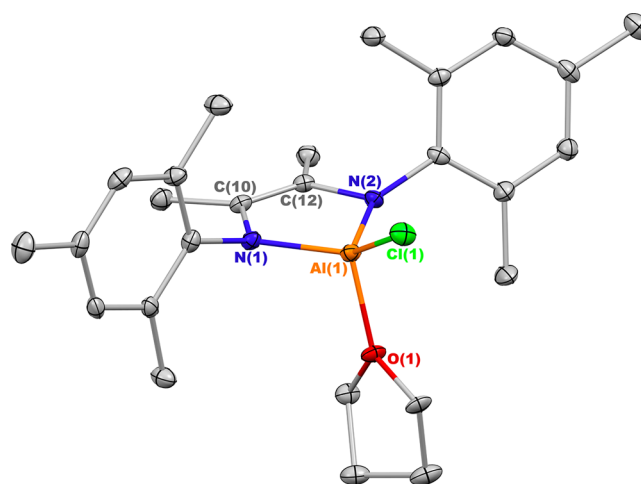


Figure 2. Solid-state structure of (L_{Mes}^{2-})AlCl(THF) (3) with ellipsoids at the 30% probability level. H atoms and an interstitial toluene molecule have been omitted for clarity.

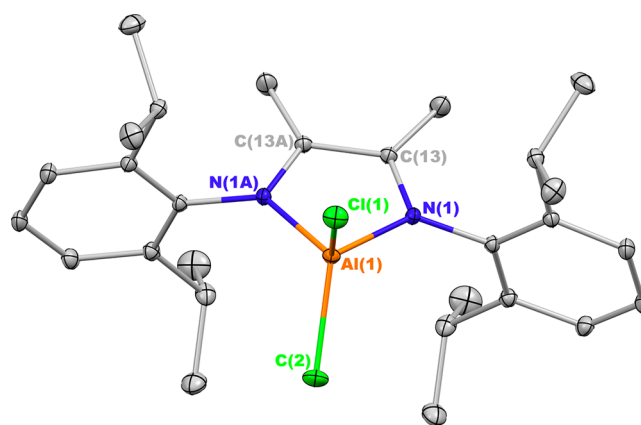


Figure 3. Solid-state structure of (L_{Dipp}^-)AlCl₂ (4). Ellipsoids are projected at 30% probability, and H atoms are omitted for clarity.

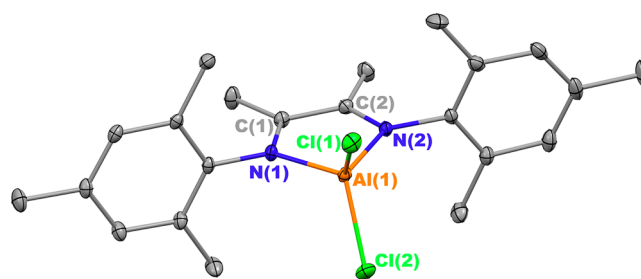


Figure 4. Solid-state structure of (L_{Mes}^-)AlCl₂ (5). Ellipsoids are projected at 30% probability, and H atoms are omitted for clarity.

for four-coordinate aluminum(III) complexes.³⁶ The Al–N bond lengths are slightly shorter for complex 3 (1.799(3) and 1.803(3) Å), which contains a doubly reduced ligand, versus complexes 4 (1.8733(9) Å) and 5 (1.8643(14) and 1.8782(15) Å), which have singly reduced ligands, supporting a relatively larger electron density on the doubly reduced ligand. A similar trend was observed for the iminopyridine complexes reported by Berben, where the N_{imido}–Al bond distances were in the range 1.806(1)–1.879(2) Å for the doubly reduced ligands relative to 1.856(1)–1.989(3) Å for the singly reduced ligands.^{19,20,22} The aluminum complexes with the Dipp-BIAN

Table 1. Crystallographic Data for Complexes 3–5

	3	4	5
formula	C ₃₃ H ₄₄ AlClN ₂ O	C ₂₈ H ₄₀ AlCl ₂ N ₂	C ₂₂ H ₂₈ AlCl ₂ N ₂
<i>a</i> (Å)	23.107(3)	12.3683(4)	17.6845(14)
<i>b</i> (Å)	11.7175(14)	21.3523(8)	14.1011(10)
<i>c</i> (Å)	23.314(3)	10.4652(4)	18.3747(14)
α (deg)	90	90	90
β (deg)	100.299(7)	90	90
γ (deg)	90	90	90
<i>V</i> (Å ³)	6210.9(12)	2763.77(17)	4582.1(6)
<i>Z</i>	8	4	8
<i>fw</i> (g/mol)	547.13	502.50	418.34
Space group	<i>C2/c</i>	<i>Pnma</i>	<i>Pbca</i>
<i>T</i> (K)	120(2)	100(2)	100(2)
λ (Å)	0.71073	0.71073	0.71073
<i>D</i> _{calc} (mg·m ⁻³)	1.170	1.208	1.213
μ (mm ⁻¹)	0.178	0.285	0.331
<i>R</i> ₁ (<i>I</i> > 2 σ (<i>I</i>))	0.0661	0.0387	0.0430
<i>wR</i> ₂ (all data)	0.1438	0.1108	0.1152
<i>T</i> _{max} / <i>T</i> _{min}	1.18	1.03	1.13
GOF (<i>F</i> ²)	1.019	1.025	1.044

ligand reported by Fedushkin also show a similar trend in bonding parameters: The Al–N lengths in the (Dipp-BIAN[−])AlCl₂ complex are 1.890(2) and 1.888(2) Å, compared to 1.844(4) and 1.838(4) Å for the [(Dipp-BIAN^{2−})AlCl₂][−] anion.³⁰

The oxidation state of the ligand could be further assessed through the bonding metrics of the N–C–C–N backbone in the complexes.³⁷ In the free L_{Mes} ligand **1**, the C–N bond lengths are 1.278(2) Å, while the C–C bond distance is 1.500(2) Å.³⁰ In comparison, there is a lengthening of the C–N bonds and shortening of the C–C bonds in the singly reduced complex **5**, supporting addition of electron density into the LUMO of the ligand.^{28b} The imido C–N bond lengths in **5** are 1.355(2) and 1.348(2) Å, and the C–C bond distance is 1.432(2) Å. Similar bonding metrics were observed for compound **4**, which has an imido C–N distance of 1.3456(13) Å and a C–C distance of 1.466(2) Å. These bond distances compare well to the metrics obtained for the [(L[−])Ca(μ_2 -Cl)(THF)₂]₂ complexes reported by Yang and co-

workers.^{25d} When L[−] is L_{Mes}[−], the imido C–N distances are 1.323(3) and 1.347(3) Å with a C–C distance of 1.432(3) Å, compared to imido C–N distances of 1.473(4) and 1.379(4) Å and a C–C distance of 1.354(4) Å when L[−] is L_{Dipp}[−]. The binding metrics are also in good agreement with those found for the (L_{Dipp}[−])AlEt₂ complex, which had imido C–N distances of 1.375(3) and 1.390(3) Å and a C–C distance of 1.391(3) Å.³²

In **3**, the α -diimine ligand exists in the enediamide form, with elongated imido C–N bond lengths of 1.438(4) and 1.440(4) Å and a shortened C–C distance of 1.341(4) Å. These bonding parameters are comparable to those reported for other complexes incorporating L_{Mes} in the doubly reduced state. The (L_{Mes}^{2−})Mg(THF)₃ complex reported by Yang, Wu, and co-workers had C–N distances of 1.426(3) and 1.406(3) Å and a C–C distance of 1.350(3) Å,^{25c} while their [Na-(THF)₂(L_{Mes}^{2−})Na]₂ complex had C–N distances of 1.428(4) and 1.411(4) Å and a C–C distance of 1.356(4) Å.^{25c}

Density Functional Theory (DFT) Studies. The full geometries of compounds **3** and **5** were optimized using DFT (Figures S6 and S7 and Tables S1 and S2) with the geometry of compound **5** constrained to C_{2v} symmetry. The theoretical bond distances and angles were found to be in good agreement with those obtained in the X-ray analysis (Table 2). As with the X-ray data, the theoretical picture shows a shortening of the C–C bond and a lengthening of the C–N bonds within the diimine backbone as additional electrons are added to the ligand system. This assertion is supported by analysis of the frontier orbitals: The HOMO of **3** and the SOMO of **5** (Figure 5) are primarily ligand based and located on the N–C–C–N backbone with a bonding interaction between the C–C and an antibonding interaction between the C–N groups.

The charge distribution of complexes **3** and **5** was studied by the natural bonding orbital (NBO) method, with selected data given in Table 3. NBO studies show that the α -diimine ligand on complex **3** is anionic, as the electron acceptors N(1) and N(2) acquire much of the negative charge, while the aluminum(III) cation has a larger positive charge. In comparison, N(1) and N(2) on complex **5** have less negative charge, as is expected for the singly reduced complex.

Table 2. Selected Calculated and Experimental Bond Distances (Å) and Angles (deg) for 3–5

	3 _{exp}	3 _{theory}	4 _{exp}	5 _{exp}	5 _{theory}
Al–N	1.799(3) 1.803(3)	1.815 1.817	1.8733(9)	1.8643(14) 1.8782(15)	1.896
Al–Cl	2.1229(14)	2.124	2.1278(6) 2.1078(6)	2.1215(7) 2.1252(7)	2.132 2.131
Al–O	1.856(2)	1.928	n/a	n/a	n/a
C–C _{backbone}	1.341(4)	1.363	1.466(2)	1.438(2)	1.422
C–N _{imine}	1.438(4) 1.440(4)	1.427 1.429	1.3456(13)	1.355(2) 1.348(2)	1.349
N–Al–N	93.45(13)	93.215	86.77(6)	87.00(6)	86.381
N–Al–Cl	122.38(11) 121.29(10)	125.045 125.160	113.44(3) 116.14(3)	114.07(5) 117.38(5) 115.24(5) 114.33(5)	114.599
N–Al–O	108.52(12) 110.50(12)	106.193 105.892	n/a	n/a	n/a
Cl–Al–Cl	n/a	n/a	109.50(3)	107.95(3)	110.368
Cl–Al–O	100.51(9)	99.450	n/a	n/a	n/a

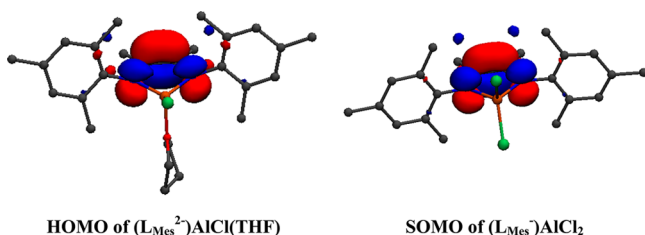


Figure 5. HOMO of $(L_{\text{Mes}}^{2-})\text{AlCl}(\text{THF})$ (3) and SOMO of $(L_{\text{Mes}}^-)\text{AlCl}_2$ (5). Molecular orbitals are visualized using VMD with isosurfaces at ± 0.03 au.

Electrochemistry. Electrochemical characterization of 3 in THF solution with 0.1 M $[n\text{-Pr}_4\text{N}][\text{BAR}^{\text{F}}]$ ($\text{BAR}^{\text{F}-} = \text{B}(3,5\text{-CF}_3)_2\text{-C}_6\text{H}_3_4^-$) supporting electrolyte showed multiple redox processes in the cyclic voltammogram (Figure 6 and Table 4). The rest potential of the complex was -1.25 V, so we assign the reversible feature centered at $E_{1/2} = -0.94$ V versus Fc/Fc^+ as an oxidation process corresponding to the L^{2-}/L^- couple. We assign the second, less reversible feature at -0.03 V as the L^-/L^0 couple. The identity of the feature at ~ -0.64 V (marked with an *) is as yet unclear, but we speculate that it is the result of a chemical process or instability of 3 under the experimental conditions. The feature was persistent across several measured samples and was observed for analytically pure material.

The cyclic voltammograms of compounds 4 and 5 are shown in Figure 7 and are cleaner than that for 3, with both compounds displaying two independent redox features. Both complexes have a reversible feature that we assign to the L^{2-}/L^- couple at $E_{1/2} = -1.37$ V (for 4) and $E_{1/2} = -1.34$ V (for 5) versus Fc/Fc^+ . Comparison of these features to that in 3 shows a shift to more reducing potentials by ~ 0.40 V. A similar shift was observed by Berben when comparing the $(\text{IP}^-)_2\text{AlCl}$ and $[\text{Na}(\text{DME})_3][(\text{IP}^{2-})_2\text{Al}]$ complexes.²¹ Complexes 4 and 5 also have processes that we assign to the L^-/L^0 couple at $E_{1/2} = -0.62$ V and $E_{1/2} = -0.73$ V versus Fc/Fc^+ , respectively. The process is quasi-reversible for 4 and reversible for 5 and more clearly defined than the corresponding feature for complex 3. Again a shift to more negative potentials was observed.

CONCLUSIONS

We have demonstrated that the redox-active α -diimine ligands can be coordinated to an aluminum(III) ion to afford complexes in the -1 or -2 oxidation state of the ligand. The structural and theoretical characterization of the complexes corroborates ligand oxidation state assignment. The electrochemical characterization shows reversible redox properties for all complexes, suggesting that the aluminum(III) ion can support all oxidation states of the ligand. We have also shown that the $(L_{\text{Mes}}^{2-})\text{AlCl}(\text{THF})$ can be oxidized using either AgCl or CuCl to give $(L_{\text{Mes}}^-)\text{AlCl}_2$, indicating the redox properties of the complex can be coupled to reactivity at the aluminum(III) ion. We are currently investigating other reactivity profiles for the complexes, namely through the development of two-electron chemistry. We are also exploring the coordination

Table 3. Charge Distribution of Complexes 3 and 5

	Al	Cl(1)	Cl(2)/O(1)	C(1)	C(2)	N(1)	N(2)
3	+1.88804	-0.53781	-0.72058	+0.09444	+0.10113	-0.98492	-0.98270
5	+1.67783	-0.53048	-0.53048	+0.23157	+0.23157	-0.78159	-0.78159

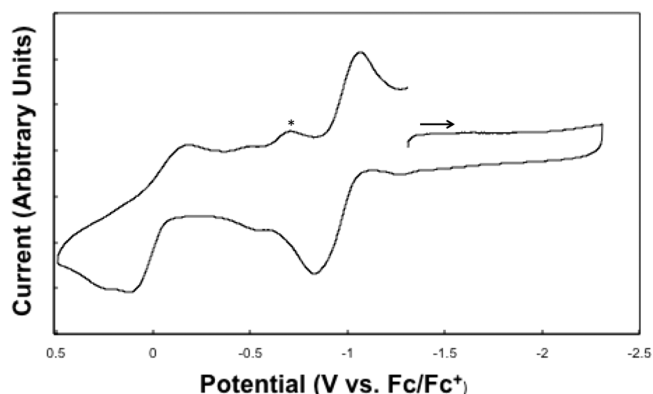


Figure 6. Cyclic voltammogram of compound 3 recorded in 0.1 M $[n\text{-Pr}_4\text{N}][\text{BAR}^{\text{F}}]$ THF solution.

Table 4. Electrochemical Potentials (V vs Fc/Fc^+) for Complexes 3–5

	diimine ²⁻ /diimine ⁻	diimine ⁻ /diimine ⁰	ΔE
3	-0.94	-0.03	0.91
4	-1.37	-0.62	0.75
5	-1.34	-0.73	0.61

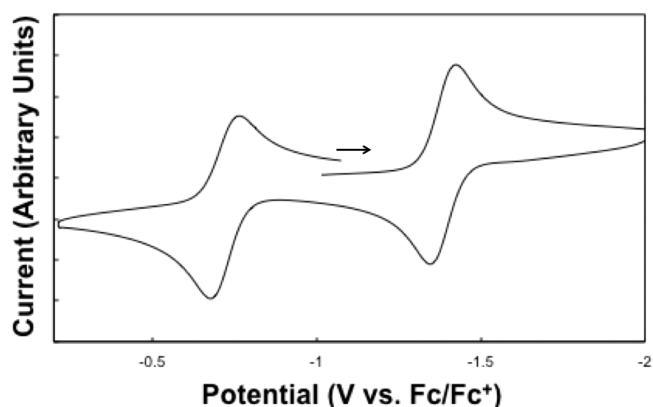
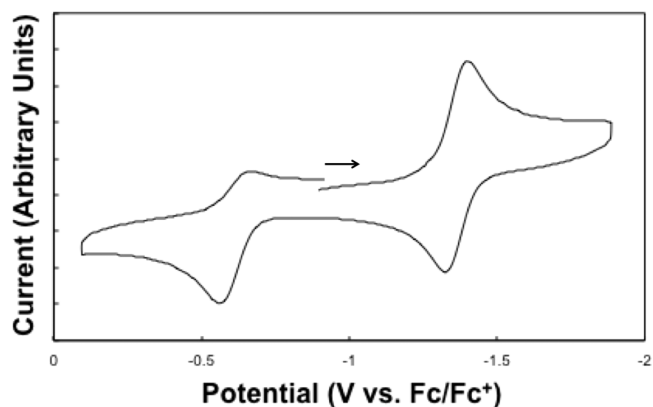


Figure 7. Cyclic voltammograms of compounds 4 (top) and 5 (bottom) recorded in 0.1 M $[n\text{-Pr}_4\text{N}][\text{BAR}^{\text{F}}]$ THF solution.

chemistry of *N*-aryl α -diimines that lack substitution in the 2,6 positions of the aryl substituent to aluminum(III) to prepare stable complexes incorporating the neutral oxidation state of the ligand.

EXPERIMENTAL SECTION

Physical Measurements. ^1H and ^{13}C NMR spectra were recorded at ambient temperature in C_6D_6 using a Varian 400 MHz spectrometer (399.78 MHz for ^1H , 100.52 MHz for ^{13}C). Chemical shifts were referenced to residual solvent. Elemental analyses were performed at the University of California, Berkeley Microanalytical Facility, on a Perkin-Elmer Series II 2400 CHNS analyzer.

Electrochemical Measurements. CVs were recorded in a glovebox under a dinitrogen environment using either a BASI Epsilon-EC potentiostat/galvanostat (for **3**) or a CH Instruments 620D electrochemical analyzer/workstation (for **4** and **5**). In both cases, a glassy carbon working electrode, a platinum wire auxiliary electrode, and a silver wire plated with AgCl as a quasi-reference electrode were utilized. Potentials were reported versus ferrocene, which was added as an internal standard for calibration at the end of each run. Solutions employed during these studies were ~ 3 mM in analyte and 100 mM in $[\eta\text{-Pr}_4\text{N}][\text{BAR}^{\text{F}}]$ ($\text{BAR}^{\text{F}-} = \text{B}(3,5\text{-CF}_3)_2\text{-C}_6\text{H}_3)_4^-$) in ~ 3 mL of THF. All data were collected in a positive-feedback IR compensation mode.

X-ray Structure Determination. X-ray diffraction data were collected on a Bruker-AXS Kappa APEX II CCD diffractometer with 0.71073 Å Mo $K\alpha$ radiation. Cell parameters were retrieved using APEX II software³⁸ and further refined on all observed reflections during integration using SAINT+.³⁹ Each data set was treated with SADABS⁴⁰ absorption corrections based on redundant multiscan data. The structures were solved by direct methods and refined by least-squares method on F^2 using the SHELXTL program package.⁴¹ All non-hydrogen atoms were refined with anisotropic displacement parameters, and all hydrogen atoms were treated with a riding model. Details regarding specific solution refinement for each compound are provided in the following paragraphs.

X-ray structural analysis for **3**: A single colorless plate ($0.2 \times 0.06 \times 0.02$ mm³) was mounted in immersion oil onto a glass fiber, and data were collected under a nitrogen stream at 120 K. Systematic absences in the data were consistent with the centrosymmetric, monoclinic space group $C2/c$. The asymmetric unit contains one ($\text{L}_{\text{Mes}}^{2-}$)AlCl₂(THF) molecule and a molecule of toluene solvent. The toluene solvent was disordered over two positions, which were located from the difference map and refined using SIMU, DELU, and SAME commands within SHELXL.

X-ray structural analysis for **4**: A single orange block ($0.2 \times 0.12 \times 0.10$ mm³) was mounted in immersion oil onto a glass fiber, and data were collected under a nitrogen stream at 100 K. Systematic absences in the data were consistent with the centrosymmetric, orthorhombic space group $Pnma$. The asymmetric unit contains one-half molecule of ($\text{L}_{\text{Dipp}}^{2-}$)AlCl₂, as the molecule lies on a crystallographic mirror plane.

X-ray structural analysis for **5**: A single orange shard ($0.27 \times 0.18 \times 0.07$ mm³) was mounted in immersion oil onto a glass fiber, and data were collected under a nitrogen stream at 100 K. Systematic absences in the data were consistent with the centrosymmetric, orthorhombic space group $Pbca$. The asymmetric unit contains one molecule of ($\text{L}_{\text{Mes}}^{2-}$)AlCl₂.

Computational Details. The structure optimization of **3** and **5** was performed with the Gaussian '09, Revision A.1,⁴² program using the M06 density functional⁴³ and the 6-31+G(d,p) basis set.^{44,45} Geometry operations were carried out in C_1 symmetry for compound **3** and C_{2v} symmetry for compound **5**. All frequency calculations found no imaginary frequencies, confirming that the optimized structures were minima. Binding analysis was performed using NBO 3 as coded within Gaussian '09. Molecular orbitals were visualized using Visual Molecular Dynamics⁴⁶ with isosurfaces at ± 0.03 au.

Preparation of Compounds. All reactions and manipulations were performed under an inert atmosphere (N_2) using standard Schlenk techniques or in a Vacuum Atmospheres, Inc. Nexus II drybox

equipped with a molecular sieves 13X/Q5 Cu-0226S catalyst purifier system. Glassware was dried overnight at 150 °C before use. C_6D_6 was purchased from Sigma Aldrich and was stored over potassium metal prior to use. Tetrahydrofuran, hexanes, pentane, and toluene were purchased from Fisher Scientific. These solvents were sparged for 20 min with dry argon and dried using a commercial two-column solvent purification system comprising columns packed with Q5 reactant and neutral alumina, respectively (for hexanes, toluene, and pentane), or two columns of neutral alumina (for THF). Celite was purchased from Sigma Aldrich and was dried under reduced pressure at 250 °C for 48 h prior to use. The α -diimine ligands L_{Mes} (**1**) and L_{Dipp} (**2**) were prepared according to literature procedures.⁴⁷ $[\eta\text{-Pr}_4\text{N}][\text{BAR}^{\text{F}}]$ was prepared as reported by Kiplinger et al.⁴⁸ All other reagents were purchased from commercial sources and used as received.

($\text{L}_{\text{Mes}}^{2-}$)AlCl₂(THF) (**3**). L_{Mes} (1.0 g, 3.12 mmol) in THF (10 mL) was added to a stirring suspension of sodium metal (0.14 g, 6.24 mmol) in THF (25 mL). After 4 h, AlCl₃ (0.42 g, 3.12 mmol) was added, and the reaction was allowed to stir at room temperature. After 12 h, the reaction was filtered over a Celite-padded frit, and volatiles were removed from the pale yellow filtrate under vacuum. The crude reaction product was taken up into toluene (50 mL) and filtered over a Celite-padded frit, and volatiles were removed from the filtrate. The resultant oily solid was tritiated with pentane (3×10 mL) and dried under reduced pressure to give **3** as an off-white solid. Yield: 1.15 g (81%). Crystals suitable for X-ray diffraction were obtained from cooling a saturated toluene solution at -25 °C. ^1H NMR: δ 6.96 (s, 4H), 3.45 (bm, 4H, THF), 2.69 (bs, 6H, *o*-CH₃), 2.32 (bs, 6H, *o*-CH₃), 2.26 (s, 6H, *p*-CH₃), 1.78 (s, 6H, CH₃-C-N), 0.78 (bs, 4H, THF). $^{13}\text{C}\{^1\text{H}\}$ NMR: δ 166.4, 144.2, 132.7, 128.1, 118.6, 73.2, 25.2, 21.6, 20.4, 14.6. Anal. Calcd for $\text{C}_{26}\text{H}_{36}\text{AlCl}_2\text{N}_2\text{O}$: C, 68.63; H, 7.98; N, 6.16. Found: C, 68.56; H, 7.82; N, 6.00.

($\text{L}_{\text{Dipp}}^{2-}$)AlCl₂ (**4**). L_{Dipp} (0.50 g, 1.23 mmol) in THF (10 mL) was added to a stirring suspension of sodium metal (0.028 g, 1.23 mmol) in THF (25 mL). After 4 h, AlCl₃ (0.16 g, 1.23 mmol) was added, and the reaction was allowed to stir at room temperature. After 12 h, the reaction was filtered over a Celite-padded frit, and volatiles were removed from the pale yellow filtrate under vacuum. The crude reaction product was taken up into hot toluene (25 mL) and filtered over a Celite-padded frit, and volatiles were removed from the filtrate. Yield: 0.48 g (77%). Crystals suitable for X-ray diffraction were obtained from cooling a saturated hexane solution at -25 °C. Anal. Calcd for $\text{C}_{28}\text{H}_{40}\text{AlCl}_2\text{N}_2$: C, 66.92; H, 8.02; N, 5.57. Found: C, 67.45; H, 8.07; N, 5.25.

($\text{L}_{\text{Mes}}^{2-}$)AlCl₂ (**5**). Using AgCl: ($\text{L}_{\text{Mes}}^{2-}$)AlCl₂(THF) (**3**) (0.50 g, 1.10 mmol) was dissolved in toluene (25 mL), and AgCl (0.16 g, 1.10 mmol) was added. The solution was stirred at room temperature for 12 h, after which it was filtered over a Celite-padded frit, and volatiles were removed from the orange filtrate under vacuum. The crude reaction product was taken up into boiling hexanes (25 mL) and filtered over a Celite-padded frit, and volatiles were removed from the filtrate to give **5** as an orange powder. Yield: 0.41 g (89%).

Using CuCl: ($\text{L}_{\text{Mes}}^{2-}$)AlCl₂(THF) (**3**) (0.25 g, 0.55 mmol) was dissolved in toluene (15 mL), and CuCl (0.055 g, 0.55 mmol) was added. The solution was stirred at room temperature for 3 h, after which it was filtered over a Celite-padded frit, and volatiles were removed from the orange filtrate under vacuum. The crude reaction product was taken up into boiling hexanes (25 mL) and filtered over a Celite-padded frit, and volatiles were removed from the filtrate to give **5** as an orange powder. Yield: 0.15 g (65%).

Crystals suitable for X-ray diffraction were obtained from cooling a saturated hexane solution at -25 °C. Anal. Calcd for $\text{C}_{22}\text{H}_{28}\text{AlCl}_2\text{N}_2$: C, 63.16; H, 6.75; N, 6.70. Found: C, 62.32; H, 6.63; N, 6.32.

ASSOCIATED CONTENT

Supporting Information

^1H NMR spectra of **3**–**5**. VT-NMR spectra for **3**. ^{13}C NMR spectrum of **3**. Tables of coordinates from geometry optimizations of **3** and **5**. Full ref 42. CIF files for complexes

3–5. This material is available free of charge via the Internet at <http://pubs.acs.org>.

AUTHOR INFORMATION

Corresponding Author

*E-mail: cgraves@alb.edu.

Notes

The authors declare no competing financial interest.

ACKNOWLEDGMENTS

We thank Albright College and the ACS-Petroleum Research Fund (PRF 52181-UNI3) for financial support of this work. We thank the George I. Alden Trust for funding toward the NMR spectrometer used in this work. B.E.C. thanks Albright College for a 2012 Summer Research Fellowship and the Goldwater Foundation. We thank Jerome Robinson and Professor Eric J. Schelter (both University of Pennsylvania) for helpful discussions.

REFERENCES

- (1) Rosner, H. (Oct 15, 2012) A Chemist Comes Very Close to a Midas Touch. The New York Times. Retrieved from <http://www.nytimes.com/2012/10/16/science/modern-day-alchemy-has-iron-working-like-platinum.html?pagewanted=all>.
- (2) Rabinovich, D. *Nat. Chem.* **2013**, *5*, 76.
- (3) Cotton, F. A.; Wilkinson, G.; Murillo, C. A.; Bochmann, M. *Advanced Inorganic Chemistry*, 6th ed.; John Wiley & Sons, Inc.: New York, 1999.
- (4) *Aluminum*; U.S. Geological Survey: Reston, VA, December 2013.
- (5) Haynes, W. M., Ed. *CRC Handbook of Chemistry and Physics*, 91st ed. CRC: Boca Raton, FL, 2010; pp 4-1–4-42.
- (6) Taguchi, T.; Yanai, H. Al(III) Lewis Acids. In *Acid Catalysis in Modern Organic Synthesis*; Yamamoto, H.; Ishihara, K., Eds.; Wiley-VCH: New York, 2008; Vol. 1, pp 241–345.
- (7) Cui, C.; Roesky, H. W.; Schmidt, H.-G.; Noltemeyer, M.; Hao, H.; Cimpoesu, F. *Angew. Chem., Int. Ed.* **2000**, *39*, 4274–4276.
- (8) Zhu, H.; Chai, J.; Chandrasekhar, V.; Roesky, H. W.; Magull, J.; Vidovic, D.; Schmidt, H.-G.; Noltemeyer, M.; Power, P. P. *J. Am. Chem. Soc.* **2004**, *126*, 9472–9473.
- (9) Zhu, H.; Chai, J.; Stasch, A.; Roesky, H. W.; Blunck, T.; Vidovic, D.; Magull, J.; Schmidt, H.-G.; Noltemeyer, M. *Eur. J. Inorg. Chem.* **2004**, 4046–4051.
- (10) Dohmeier, C.; Robl, C.; Tacke, M.; Schnoekel, H. *Angew. Chem., Int. Ed.* **1991**, *30*, 564–565.
- (11) Purath, A.; Dohmeier, C.; Ecker, A.; Schnoekel, H.; Amelunxen, K.; Passler, T.; Wiberg, N. *Organometallics* **1998**, *17*, 1894–1896.
- (12) Purath, A.; Schnoekel, H. *J. Organomet. Chem.* **1999**, *579*, 373–375.
- (13) Schnitter, C.; Roesky, H. W.; Ropken, C.; Herbst-Irmer, R.; Schmidt, H.-G.; Noltemeyer, M. *Angew. Chem., Int. Ed.* **1998**, *37*, 1952–1955.
- (14) Schulz, S.; Roesky, H. W.; Koch, H. J.; Sheldrick, G. M.; Stalke, D.; Kuhn, A. *Angew. Chem., Int. Ed.* **1993**, *32*, 1729–1731.
- (15) Sitzmann, H.; Lappert, M. F.; Dohmeier, C.; Uffing, C.; Schnoekel, H. *J. Organomet. Chem.* **1998**, *561*, 203–208.
- (16) For seminal examples, see: (a) Bart, S. C.; Lobkovsky, E.; Chirik, P. J. *J. Am. Chem. Soc.* **2004**, *126*, 13794–13807. (b) Blackmore, K. J.; Ziller, J. W.; Heyduk, A. F. *Inorg. Chem.* **2005**, *44*, 5559–5561. (c) Bart, S. C.; Hawrelak, E. J.; Lobkovsky, E.; Chirik, P. J. *Organometallics* **2005**, *24*, 5518–5527. (d) Haneline, M. R.; Heyduk, A. F. *J. Am. Chem. Soc.* **2006**, *128*, 8410–8411. (e) Blackmore, K. J.; Lal, N.; Ziller, J. W.; Heyduk, A. F. *J. Am. Chem. Soc.* **2008**, *130*, 2728–2729. (f) Hess, C. R.; Weyhermuller, T.; Bill, E.; Wieghardt, K. *Inorg. Chem.* **2010**, *49*, 5686–5700. (g) Nguyen, A. L.; Zarkesh, R. A.; Lacy, D. C.; Thorson, M. K.; Heyduk, A. F. *Chem. Sci.* **2011**, *2*, 166–169. (h) Khusniyarov, M. M.; Bill, E.; Weyhermuller, T.; Bothe, E.; Wieghardt, K. *Angew. Chem., Int. Ed.* **2011**, *50*, 1652–1655. (i) Darmon, J. M.; Stieber, S. C. E.; Sylvester, K. T.; Fernandez, I.; Lobkovsky, E.; Semproni, S. P.; Bill, E.; Wieghardt, K.; DeBeer, S.; Chirik, P. J. *J. Am. Chem. Soc.* **2012**, *134*, 17125–17137.
- (17) For recent reviews on the application of redox-active ligand metal complexes in catalysis, see: (a) Lyaskovskyy, V.; de Bruin, B. *ACS Catal.* **2012**, *2*, 270–279. (b) Luca, O. R.; Crabtree, R. H. *Chem. Soc. Rev.* **2013**, *42*, 1440–1459.
- (18) For recent reviews, see: (a) Kaim, W. *Eur. J. Inorg. Chem.* **2012**, *2012*, 343–348. Caulton, K. G. *Eur. J. Inorg. Chem.* **2012**, *2012*, 435–443.
- (19) Myers, T. W.; Berben, L. A. *J. Am. Chem. Soc.* **2011**, *133*, 11865–11867.
- (20) Myers, T. W.; Holmes, A. L.; Berben, L. A. *Inorg. Chem.* **2012**, *51*, 8997–9004.
- (21) Myers, T. W.; Kazem, N.; Stoll, S.; Britt, R. D.; Shanmugam, M.; Berben, L. A. *J. Am. Chem. Soc.* **2011**, *133*, 8662–8672.
- (22) Myers, T. W.; Berben, L. A. *Inorg. Chem.* **2012**, *51*, 1480–1488.
- (23) Myers, T. W.; Berben, L. A. *Chem. Commun.* **2013**, *49*, 4175–4177.
- (24) Chirik, P. J. *Inorg. Chem.* **2011**, *50*, 9737–9740.
- (25) For recent examples, see: (a) Hinchliffe, A.; Mair, F. S.; McInnes, E. J. L.; Pritchard, R. G.; Warren, J. E. *Dalton Trans.* **2008**, 222–233. (b) Yu, J.; Yang, X.-J.; Liu, Y.; Pu, Z.; Li, Q.-S.; Xie, Y.; Schaefer, H. F.; Wu, B. *Organometallics* **2008**, *27*, 5800–5805. (c) Liu, Y.; Yang, P.; Yu, J.; Yang, X.-J.; Zhang, J. D.; Chen, Z.; Schaefer, H. F.; Wu, B. *Organometallics* **2008**, *27*, 5830–5835. (d) Liu, Y.; Zhao, Y.; Yang, X.-J.; Li, S.; Gao, J.; Yang, P.; Xia, Y.; Wu, B. *Organometallics* **2011**, *30*, 1599–1606. (e) Panda, T. K.; Kaneko, H.; Michel, O.; Pal, K.; Tsurugi, H.; Tornroos, K. W.; Anwender, R.; Mashima, K. *Organometallics* **2012**, *31*, 3178–3184. (f) Lorenz, V.; Hrib, C. G.; Grote, D.; Hilfert, L.; Krasnopolski, M.; Edelmann, F. T. *Organometallics* **2013**, *32*, 4636–4642.
- (26) For recent examples, see: (a) Ghosh, M.; Sproules, S.; Weyhermuller, T.; Wieghardt, K. *Inorg. Chem.* **2008**, *47*, 5963–5970. (b) Muresan, N.; Lu, C. C.; Ghosh, M.; Peters, J. C.; Abe, M.; Henling, L. M.; Weyhermuller, T.; Bill, E.; Wieghardt, K. *Inorg. Chem.* **2008**, *47*, 4579–4590. (c) Kreisel, K. A.; Yap, G. P. A.; Theopold, K. H. *Eur. J. Inorg. Chem.* **2012**, *2012*, 520–529. (d) Zhang, D.; Nadres, E. T.; Brookhart, M.; Daugulis, O. *Organometallics* **2013**, *32*, 5136–5143. (e) Yang, X.-J.; Fan, X.; Zhao, Y.; Wang, X.; Liu, B.; Su, J.-H.; Dong, Q.; Xu, M.; Wu, B. *Organometallics* **2013**, *32*, 6945–6949.
- (27) (a) Booth, C. H.; Walter, M. D.; Kazhdan, D.; Hu, Y.-J.; Lukens, W. W.; Bauer, E. D.; Maron, L.; Eisenstein, O.; Andersen, R. A. *J. Am. Chem. Soc.* **2009**, *131*, 6480–6491. (b) Panda, T. K.; Kaneko, H.; Pal, K.; Tsurugi, H.; Mashima, K. *Organometallics* **2010**, *29*, 2610–2615. (c) Kraft, S. J.; Williams, U. J.; Daly, S. R.; Schelter, E. J.; Kozimor, S. A.; Boland, K. S.; Kikkawa, J. M.; Forrester, W. P.; Christensen, C. N.; Schwarz, D. E.; Fanwick, P. E.; Clark, D. L.; Conradson, S. D.; Bart, S. C. *Inorg. Chem.* **2011**, *50*, 9838–9848. (d) Mrutu, A.; Barnes, C. L.; Bart, S. C.; Walensky, J. R. *Eur. J. Inorg. Chem.* **2013**, 4050–4055.
- (28) (a) Cloke, F. G. N.; Dalby, C. I.; Henderson, M. J.; Hitchcock, P. B.; Kennard, C. H. L.; Lamb, R. L.; Raston, C. L. *J. Chem. Soc., Chem. Commun.* **1990**, 1394–1396. (b) Cloke, F. G. N.; Dalby, C. I.; Daff, P. J.; Green, J. C. *J. Chem. Soc., Dalton Trans.* **1991**, 181–184.
- (29) Baker, R. J.; Farley, R. D.; Jones, C.; Kloth, M.; Murphy, D. M. *J. Chem. Soc., Dalton Trans.* **2002**, 3844–3850.
- (30) Lukoyanov, A. N.; Fedushkin, I. L.; Hummert, M.; Schumann, H. *Russ. Chem. B* **2006**, *55*, 422–428.
- (31) Schumann, H.; Hummert, M.; Lukoyanov, A. N.; Fedushkin, I. L. *Organometallics* **2005**, *24*, 3891–3896.
- (32) Li, J.; Zhang, K.; Huang, H.; Yu, A.; Hu, H.; Cui, H.; Cui, C. *Organometallics* **2013**, *32*, 1630–1635.
- (33) The $[\text{trans}-(\text{THF})_4\text{AlCl}_2]^+$ cation has been previously reported in the reaction of AlCl_3 with THF. See: Means, N. C.; Means, C. M.; Bott, S. G.; Atwood, J. L. *Inorg. Chem.* **1987**, *26*, 1466–1468.
- (34) Cui showed that the neutral ligand complex $[(\text{L}_{\text{Dipp}})\text{AlCl}_2][\text{AlCl}_4]$ could be prepared from reaction of $(\text{L}_{\text{Dipp}}^-)\text{AlEt}_2$ with BCl_3

with the reaction and crystallization being performed in non-coordinating hexanes solvent. See ref 32.

(35) A metal complex with an ideal tetrahedral geometry will have a $\tau_4 = 1.00$, while an ideal trigonal pyramidal complex will have $\tau_4 = 0.85$. See: Yang, L.; Powell, D. R.; Houser, R. P. *Dalton Trans.* **2007**, 955–964.

(36) For representative Al–Cl bond lengths in four-coordinate aluminum complexes, see: (a) Schmidt, J. A. R.; Arnold, J. *Organometallics* **2002**, *21*, 2306–2313 (Al–Cl, 2.110(1) Å, 2.111(1) Å). (b) Burford, N.; D'eon, M.; Ragogna, P. J.; McDonald, R.; Ferguson, M. *Inorg. Chem.* **2004**, *43*, 734–738 (Al–Cl, 2.1228(12) Å, 2.1007(12) Å). (c) Yang, Y.; Li, H.; Wang, C.; Roesky, H. W. *Inorg. Chem.* **2012**, *51*, 2204–2211 (Al–Cl, 2.1635(12) Å). Also see refs 22 (Al–Cl, 2.1176(6) Å, 2.115(1) Å) and 30 (Al–Cl, 2.109(1)–2.151(2) Å).

(37) Corn, I. R.; Astudillo-Sanchez, P. D.; Zdilla, M. J.; Ranwick, P. E.; Shaw, M. J.; Miller, J. T.; Evans, D. H.; Abu-Omar, M. M. *Inorg. Chem.* **2013**, *52*, 5457–5463 and references therein.

(38) APEX II, v. 2012.10-0 or v. 2013.4-1; Bruker AXS: Madison, WI, 2012.

(39) SAINT+, v. 8.26A: Data Reduction and Correction Program; Bruker AXS: Madison, WI, 2011.

(40) SADABS/TWINABS, v. 2012/1: An Empirical Absorption Correction Program; Bruker AXS Inc.: Madison, WI, 2012.

(41) Sheldrick, G. M. *SHELXTL*, v. 2012.10-2 or higher: Structure Determination Software Suite; Bruker AXS Inc.: Madison, WI, 2012.

(42) Frisch, M. J.; et al. Gaussian 09; Gaussian, Inc.: Wallingford, CT, 2009. The full reference is available in the Supporting Information.

(43) Zhao, Y.; Truhlar, D. G. *Theor. Chem. Acc.* **2008**, *120*, 215–241.

(44) Clark, T.; Chandrasekhar, J.; Spitznagel, G. W.; Schleyer, P. v. R. *J. Comput. Chem.* **1983**, *4*, 294–301.

(45) Francl, M. M.; Pietro, W. J.; Hehre, W. J.; Binkley, J. S.; Gordon, M. S.; DeFrees, D. J.; Pople, J. A. *J. Chem. Phys.* **1982**, *77*, 3654–3665.

(46) Humphrey, W.; Dalke, A.; Schulten, K. *J. Mol. Graphics* **1996**, *14*, 33–38, <http://www.ks.uiuc.edu/Research/vmd/>.

(47) van Ausdall, B. R.; Glass, J. L.; Wiggins, K. M.; Aarif, A. M.; Louie, J. J. *Org. Chem.* **2009**, *74*, 7935–7942.

(48) Thomson, R. K.; Scott, B. L.; Morris, D. E.; Kiplinger, J. L. C. R. *Chim.* **2010**, *13*, 790–802.